The effect of properties and microstructure of recycled aggregate on polypropylene fibre-reinforced concrete

Efecto de las propiedades y de la microestructura del árido reciclado en el hormigón reforzado con macrofibras de polipropileno

Guanzhi Liu[a], Josep Claramunt[b], Martin Hunger[c], Nikola Tošić[d], Albert de la Fuente[e]

[a] MSc Mining Engineering. Universitat Politècnica de Catalunya. PhD student. guanzhi.liu@upc.edu

[b] PhD Architect. Universitat Politècnica de Catalunya. Associate Professor. josep.claramunt@upc.edu

[c] PhD Civil Engineering. Master Builders Solutions. Head of Global Fiber Competence Center. martin.hunger@masterbuilders.com

[d] PhD Civil Engineering. Universitat Politècnica de Catalunya. Assistant professor. nikola.tosic@upc.edu

[d] PhD Civil Engineering. Universitat Politècnica de Catalunya. Full professor. albert.de.la.fuente@upc.edu

ABSTRACT

This study investigates the effects of different recycled aggregates on the mechanical properties and microstructure of polypropylene fibre-reinforced concrete (PPFRC). Coarse recycled aggregate (RA) and coarse recycled aggregate with embedded fibres (RAF), obtained from PPFRC recycling, were chosen for the study. The stress-strain behaviour in compression and flexural behaviour, were tested. Scanning electron microscopy (SEM) was used to examine the microstructure and elucidate the effects of different aggregates on PPFRC properties. The results indicated that RAF does not affect the compressive strength and elastic modulus but has an effect on the residual strength compared with RA.

RESUMEN

Este estudio analiza el impacto de diferentes áridos reciclados en las propiedades mecánicas y la microestructura del hormigón reforzado con fibras de polipropileno (PPFRC). Se evaluaron el árido reciclado grueso (RA) y el árido reciclado grueso con fibras embebidas (RAF) obtenidos del reciclado de PPFRC. Se ensayó la respuesta tensión-deformación en compresión y flexión, y se empleó microscopía electrónica de barrido (SEM) para examinar la microestructura. Los resultados muestran que el RAF no afecta la resistencia a la compresión ni el módulo elástico, pero sí la resistenci.

KEYWORDS: Recycled aggregate with embedded fibre, PPFRC, mechanical property, Microstructure

PALABRAS CLAVE: Árido reciclado con fibra embebida, PPFRC, propiedad mecánica, Microestructura.

1.Introduction

Concrete, one of the most widely used construction materials globally, has an annual production exceeding 4 billion tons worldwide. [1]. At the same time, numerous buildings and structures have been demolished in recent years due to reaching their end-of-life or other reasons, generating substantial construction and demolition waste (CDW). Presently, the optimal way to manage this waste is through recycling, which involves converting it into aggregates for reuse in concrete. Since aggregates constitute a significant portion of concrete, occupying 60–75% of its volume [2], recycling CDW as aggregate is a viable solution from a circular economy point of view. In general, recycled concrete aggregate (RCA), recycled masonry aggregate (RMA), and mixed recycled aggregate (MRA) are obtained when recycling CDW [3]. Among these, RCA is widely regarded as the most suitable for structural applications due to its relatively low water absorption and high strength.

The literature suggests that replacing natural aggregate (NA) with recycled concrete aggregate (RCA) at ratios below 30% has no significant influence on the physical and mechanical properties of concrete [4, 5]. However, when the RCA replacement rate reaches 100%, there is a varying degree of reduction in mechanical properties. Compressive strength decreases 12–25% [6–8], whereas splitting tensile and flexural strengths are reduced by 10–24% and 16–23% respectively [6, 9, 10]. These reductions occur primarily due to the lower stiffness and strength of RCA, along with its high-water absorption and porosity. Rao et al. [11] demonstrated that the loose residual mortar present in RCA creates a weak interface between the RCA and the new cement paste, thereby reducing the flexural strength of recycled aggregate concrete (RAC).

Despite the environmental and economic benefits of using recycled aggregates, their systematic implementation in concrete still faces challenges. Recycled aggregates often exhibit inferior quality compared to natural aggregates due to the presence of residual mortar and higher porosity, leading to lower strength and durability in recycled aggregate concrete [12, 13]. However, incorporating fibers into concrete has been shown to enhance its mechanical properties and toughness, which can offset some of the drawbacks associated with recycled aggregates [14]. Polypropylene fibers (PPF), in particular, have gained attention for their ability to improve post-cracking behavior and mitigate shrinkage in concrete [15]. However, research on the recycling of polypropylene fibre-reinforced concrete (PPFRC) remains in its early stages. Tošić et al. [16] found that the residual tensile strength of PPFRC using recycled aggregate with embedded fibres and fibres recovered from FRC recycling, was better than that of PPFRC using natural aggregate. However, the effect of using recycled aggregates with embedded fibres in recycled aggregate concrete is still insufficiently understood both at the macro and micro levels.

Therefore, the primary contribution of this paper is to compare the microstructure and macroscopic features of natural aggregate, recycled aggregate, and recycled aggregate embedded with fibers—originating from the recycling of polypropylene fiber-reinforced concrete (PPFRC)—in new PPFRC. The study evaluates the effects of different coarse aggregates and fiber content on mechanical properties through testing and further investigates the degree of bonding between concrete and various aggregates using scanning electron microscopy (SEM).

2. Experimental program

2.1 Materials

The natural aggregate (NA) was crushed limestone from a quarry in Vallcarca (Barcelona province, Spain) used in fractions 0/4, 4/12, and

12/20 mm. The recycled aggregate without embedded fibres (RA) and recycled aggregate with embedded fibres (RAF) were obtained by crushing a plain concrete and PPFRC, respectively, both with a compressive strength of 30 MPa. The schematic diagram of three types coarse aggregates shown in the Fig. 1. Physical properties of all the aggregates are tested according to EN 1097-6 [17] and provided in Table 1. The cement used in the study was CEM II/A-L 42.5N (Cementos Molins, Spain). MasterPozzolith 7003 (Master Builder Solutions, Germany) was used as a plasticizer. The virgin PPF was an embossed mono-filament (single-strand fibre, treated to have a textured surface) polypropylene fibre with a length of 40 mm, an aspect ratio of 49, a tensile strength of 552 MPa, and a density of 910 kg/m^3 supplied by Master Builders Solutions.

Fig 1. The schematic diagram of three types coarse aggregates: a. NA; b. RA; c. RAF

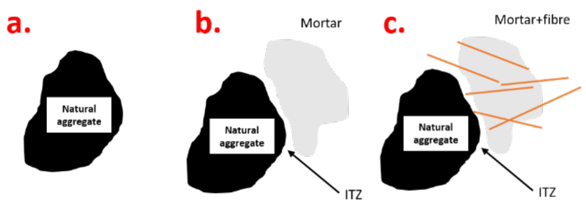

Table 1. Physical properties of the aggregate.

Type	Fraction (mm)	Fines content (%)	24 h water absorptio n (%)	Oven-dry density (kg/m³)
NA	0/4	8.1	1.56	2590
	4/12	0.5	0.57	2690
	12/20	2.4	0.61	2680
RA	0/4	5.03	6.87	2218
	4/12	0.37	5.87	2317
RAF	0/4	3.45	6.82	2269
	4/12	6.76	5.28	2310

2.2 Mix proportions and specimen preparation

Three concrete mixes were designed, the details shown in Table 2. To compare the stress-strain behaviour and the residual flexural tensile strength, all mixes maintained the same target mean compressive strength at 28 days of 30 MPa and a slump class of S3 (125 ± 25 mm). Considering the physical properties of RA and RAF, the cement dosage was increased to 385 kg/m^3 and the additional water satisfied half of the 24 h water absorption of the recycled aggregate, as indicated by the findings in [18] .

Table 2. Mix design of the tested concretes

Mix code	NA-9	RA-9	RAF-9
Cement (kg/m³)	350	385	385
w_{eff} [1] (kg/m³)	192.5	192.5	192.5
w_{add} [2] (kg/m³)	0	25.6	26.9
Plast. (wt% of cement)	1.50	1.50	1.65
0/4 mm	771.5	757.0	675.6
4/12 mm	262.1	358.7	441.7
12/20 mm	696.4	452.1	449.7

1 effective water; 2 water added for RA and RAF absorption.

For each concrete, three cylindrical specimens (Ø150×300 mm^3) and three prismatic specimens (150×150×600 mm^3) were moulded. All specimens were produced in a laboratory concrete pan mixer (Colloatic 65/2 K-3) with a capacity of 35 l. For concrete with NA, the aggregates and cement were mixed together for 60 s after which the water was added with the plasticizer and mixed for another 60 s, after which the fibre was added for another 60 s of mixing. However, for other concretes, a difference during the mixing process was the additional water that was added to the mix of fine NA and RA/RAF. When fine NA and RA/RAF were placed together in the mixer, they were first mixed for 30 s, then additional water was added and mixed for a further 30 s. The target slump value was reached for all concrete mixes.

Each cylinder was filled with concrete in three stages, each stage followed by compaction on a vibrating table, for around 10 s. Each prism was also filled in three times, and casted from the middle of the mould. During the filling process, the concrete was spread and consolidated using a vibrating table. To maintain the moist condition, the specimens were covered with a plastic sheet. After 24 h, the concrete specimens were demoulded and cured under 100 % relative humidity at a temperature of 22 °C ± 2 °C (i.e., standard curing conditions) until testing.

2.3 Test procedures

In this study, the tested items included stress-strain behavior under compression, residual flexural tensile strength, and microstructural characterization.

For the stress–strain testing, a compression testing machine (IBERTEST MEH 3000) was used. The loading rate was kept at 0.5 MPa/s until the resistance dropped to 50% of the maximum load after reaching its peak value. The applied load and resulting deformation were measured to determine the stress-strain behaviour of the concrete specimens. The compressive strength (f_c) and the elastic modulus (E_c) were also calculated based on the stress-strain curves [19].

The residual flexural tensile strength was determined using the 3-point bending test according to EN 14651 [20]. The Servohydraulic Test System (Instron 8505) was used. In order to understand the reasons for the dispersion of experimental results for certain types of fibres, the number of fibres passing through the cracked surface was determined. For this purpose, the bending test was carried out until breaking the specimen, and the sensor was removed when the crack opening displacement (CMOD) increased above 4 mm. The crack surface of each specimen was divided into four horizontal strips of equal height (1/4 of the total height each) and the number of fibres in each strip was counted. The fracture behaviour of concrete is often characterized by the fracture energy (G_f). A technique referred to as the work-of-fracture method has been developed for its determination [21, 22]

$$G_f = \frac{W_0 + mg\delta}{A} \quad (1)$$

where W_0 refers to the area underneath the load-CMOD curve (N/ m), δ is the maximum displacement (m), $m{\cdot}g$ is the self-weight of the notched beam specimen between supports (N), and A is the fracture area equal to ($b\times h_{sp}$) (m^2).

The microstructures of ITZ between cement pastes and aggregates/fibres and the surface of the fibres were investigated. The observations were conducted using Scanning Electron Microscopy (SEM) equipped with a Backscattered Electron Detector (BSEM) on a JEOL JSM 6300 microscope (Jeol Ltd.). All the specimens were taken from the broken sections that fractured during the tensile tests after standard curing at 28 days. Two types of sample were prepared. To observe the microstructure, the specimens were prepared by cutting them into prismatic shapes measuring approximately 5 × 5 × 10 mm^3 and then encapsulating them in epoxy resin. Subsequently, the sample capsules underwent sequential polishing to a degree of fineness of 1 micron using diamond paste. To observe the surface of the fibres, samples of 5 × 5 × 20 mm^3 were split just before coating.

3. Results and Discussion

3.1 Stress–strain behaviour in compression

Fig 2. shows the stress-strain curves for different concretes in compression, each curve being the average of the test results for three cylinders. All curves were divided into two parts: ascending and descending branches. For the ascending part, the type of aggregate determines the slope of the curve, which is higher for NA than for RA and RAF. This difference is due to the lower elastic modulus of RA and RAF concretes, as the recycled aggregate has a lower stiffness and provides a weaker interface between the natural aggregate and the paste. On the descending part, the curves went down after peak and the highest one was NA.

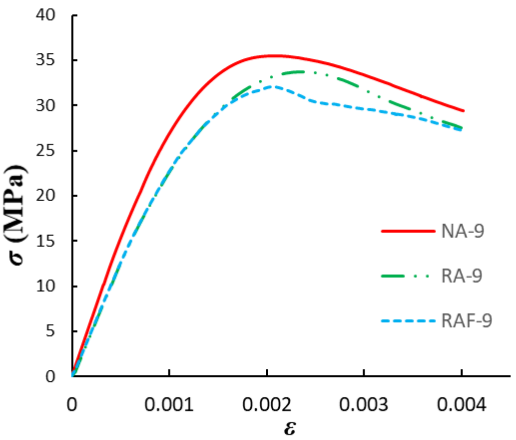

Fig. 2 Stress-strain diagram in compression of the tested concretes

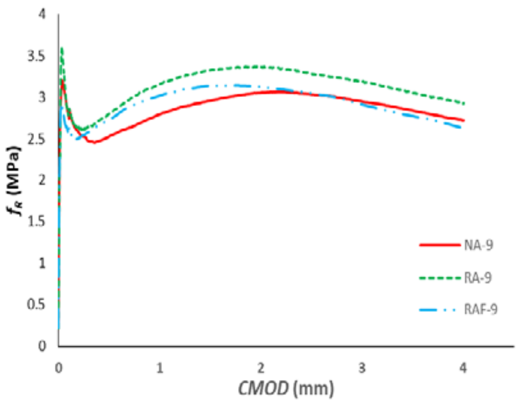

Fig. 3 Residual strength–crack mouth opening displacement curves for the tested concretes

The results for f_c and E_c are presented in Table 3. As previously mentioned, the target f_c was achieved by adjusting the mixture design, which did not differ significantly from the original. However, the E_c of RA-9 and RAF-9 were significantly lower than that of NA-9, with reductions of 15.7% and 18.1%, respectively. This indicates that, while adjusting the mixture design makes it possible to achieve the same f_c when using RA or RAF as with NA, the E_c remains lower, consistent with findings from previous study [23].

Table 3. f_c and E_c results at 28 days with CoV [%] in parentheses

	NA-9	RA-9	RAF-9
f_c	36.0 (3.0)	34.0 (4.3)	32.9 (7.8)
E_c	31.0 (1.0)	26.1 (1.0)	25.4 (1.0)

3.2 Flexural behaviour

The flexural strength-crack mouth opening displacement curves of concrete with NA, RA and RAF are plotted in Fig. 3. Each curve represents the average of three tested specimens. Due to the equal strength design, the flexural tensile strength/limit of proportionality (f_{LOP}) did not change significantly among the different concrete types. Additionally, all curves showed residual strength recovery after an initial drop following cracking. The curve of concrete produced with RA was the highest, followed by concrete produced with RAF, and finally NA. This result differed from the stress-strain behaviour in compression.

It is widely recognized that adding fibres to concrete significantly enhances its toughness[14]. Table 5 presents the residual tensile flexural strengths (f_R) and fracture energy (G_f) which were calculated according to Equation 1. The f_{LOP} values were between 3.06 and 3.45 MPa, which weren't influenced by the types of coarse aggregates. However, the residual flexural tensile strength was significantly affected by the different coarse aggregates. Among them, the f_{R1} of NA-9 was the highest, being 10.5% and 22.6% greater than those of RA-9 and RAF-9, respectively. In contrast, for f_{R3}, the highest value was observed for RA-9, followed by NA-9, with RAF-9 having the lowest value. This indicates that for reduced crack widths, the coarse aggregate played a primary role in determining performance. However, larger crack widths, both the aggregate and fibers worked together to enhance performance. RA-9 had the highest G_f value, but only 6.14% and 6.94% higher than NA-9 and RAF-9, respectively. Thus, the type of aggregate appears to have a limited impact. Nonetheless, adding fibres can enhance the toughness of concrete up to a certain fibre content. If the fibre content becomes too high, it may lead to increased air entrainment and the formation of fiber balls, which can adversely affect the bonding properties of the concrete.

Table 4. Residual flexural strengths and fracture energy with CoV [%] in parentheses

	NA-9	RA-9	RAF-9

f_{LOP}(MPa)	3.45 (6.2)	3.62 (4.4)	3.06 (20.5)
f_{R1}(MPa)	3.14 (11.2)	2.81 (23.2)	2.43 (24.9)
f_{R2}(MPa)	3.10 (10.2)	3.33 (25.1)	2.81 (22.5)
f_{R3}(MPa)	3.19 (9.0)	3.29 (25.6)	2.75 (21.8)
f_{R4}(MPa)	2.98 (10.2)	3.06 (24.9)	2.51 (21.5)
G_f (N/m)	2345.2 (6.2)	2520.2 (4.4)	2365.4 (20.5)

To examine fibre distribution, the number of fibres crossing the fracture surface of the prism after the three-point bending characterization test was counted. Typically, fibres were counted on both sides of the crack to distinguish between ruptured and pulled-out fibres, but this article only explores the influence of their number and distribution. The results presented in Fig. 4 illustrate the fibre distribution on the fracture surface, specifically focusing on different types of concrete with varying fibre densities. The result revealed similar fibre distributions in RA and RAF concrete, concentrated in the 18–33 fibres range. The number of fibers is much higher than that of NA respectively. This also explains why RA-9 and RAF-9 were higher than NA-9 for reduced crack widths (< 1.0 mm).

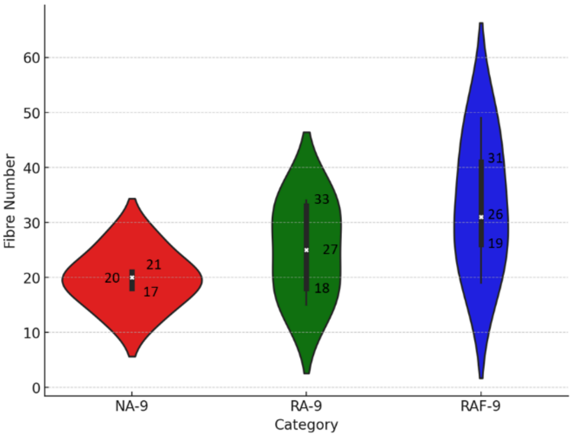

Fig. 4. Fibre distribution in each section of the fracture surface

3.3 Microstructural analysis

The mechanical properties of concrete materials are closely related to their microstructure [24]. It is generally believed that the interface bonding area between aggregate and cementitious matrix, and between fiber and cementitious material is one of the key indicators of its mechanical properties [25]. Fig. 5 shows a composition of microphotographs (A ×100 magnification and B ×750 magnification). In column 'A' of Fig. 6, the general appearance of the matrix around a fibre, identifiable by its black color, is shown. Within it, a series of uniformly gray neutral particles can be observed, which are limestone particles. These particles range from 50 to 300 µm and are marked in the images with the initials LS. These particles are surrounded by cement paste formed by smaller gray particles of different shades, which constitute Portlandite crystals along with other crystalline phases, hydrated or partially hydrated, while being surrounded by a continuous paste of a darker gray corresponding to the C-S-H phases. The latter microstructure is mainly observed in column 'B' of Fig. 6 in the three samples, where almost the entire image, except for the fibre (black color), is cement paste. In this column, a significant difference is observed between sample NA and the other two samples RA and RAF. The microstructure of sample NA is determined by a large quantity of C-S-H, forming a continuous matrix in which the rest of the particles are embedded.

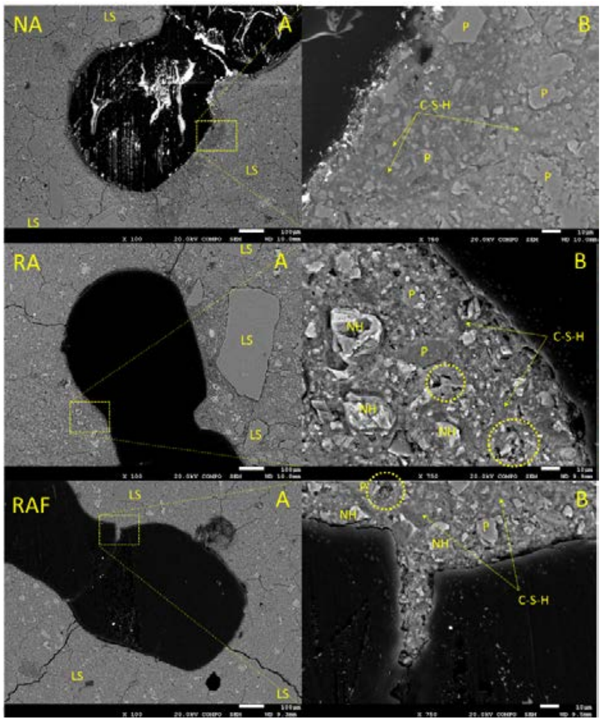

Fig. 5. Composition of microphotographs of samples NA, RA, and RAF at ×100 (A) and ×750 (B) magnification [26]**.**

Fig. 6 shows a new fibre (NF) from the fracture surface of an NA-9 sample and an embedded fibre (EF) from the RAF-9 sample. The NA-9 fibre is parallel to the fracture section and can be observed due to the detachment of a part of the surrounding matrix. Its surface exhibits the longitudinal roughness characteristic of the manufacturing process. Apart from that, only a few particles of the cement paste that have remained adhered are observed. In contrast, the embedded fibres show some surface degradation such as the longitudinal crack indicated by the letter 'F' (a similar one is also observed in the microphotograph of Fig. 9, RAF sample A and B) and superficial incisions marked with a circle of yellow dots. This damage could result in an intrinsic loss of the reinforcing capacity of the recycled fibres, which explains the mechanical properties of EF is lower than the NF.

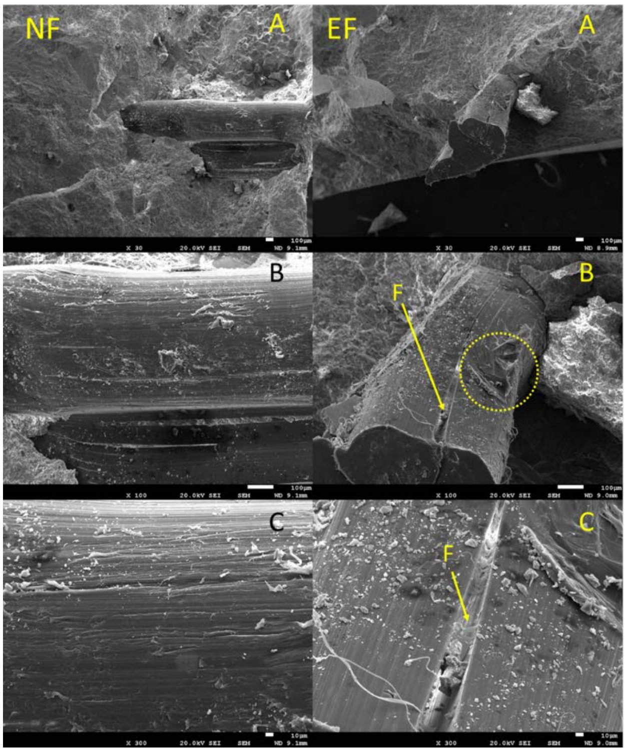

Fig. 6. Surface details of the fibres used in the experiment obtained: NF and EF [26].

4. Conclusion

The primary objective of this study was to investigate the effect of RAF on PPFRC concerning both mechanical properties and microstructure, in comparison to NA and RA. To achieve this, uniaxial stress-strain behavior under compression and flexural behavior were tested, followed by a comparative analysis of the three types of aggregate concrete. Additionally, the microstructure was analyzed using SEM to elucidate the impact of different aggregates on PPFRC. Based on this investigation, the following conclusions can be drawn:

- The results of the mechanical properties test indicate that the compressive strength and elastic modulus are not influenced by the embedded recycled fibre. However, it does affect the flexural behavior;
- The number and distribution of fibre significantly impact the flexural behaviour, however, embedded fibres in RAF may lead to adverse effects at higher fibre contents;
- The microphotographs and chemical dot mapping reveal significant differences in the composition and distribution of phases among the samples. In particular, the RAF samples exhibit unique features at the interface between recycled aggregate and new cement paste, indicating variations in hydration and porosity compared to NA and RA samples.

It is important to note that this study was conducted on a limited number of samples and only varied a limited number of parameters. Given this and the scatter in results observed in some cases, the conclusions drawn in this paper are only valid for the range of parameters tested herein. Further research is needed to confirm or refute the authors' conclusions.

Acknowledgments

This study has been supported by HEAT (PID2023-149321OB-C32), the China Scholarship Council (CSC) grant number 202106930007 and Master Builders Solutions.

References

[1] Adesina A, Zhang J (2024) Impact of concrete structures durability on its sustainability and climate resiliency. Next Sustainability 3:100025.

https://doi.org/10.1016/j.nxsust.2024.100025
[2] Behera M, Bhattacharyya SK, Minocha AK, et al (2014) Recycled aggregate from C&D waste & its use in concrete – A breakthrough towards sustainability in construction sector: A review. Construction and Building Materials 68:501–516. https://doi.org/10.1016/j.conbuildmat.2014.07.003
[3] Silva RV, de Brito J, Dhir RK (2016) Performance of cementitious renderings and masonry mortars containing recycled aggregates from construction and demolition wastes. Construction and Building Materials 105:400–415. https://doi.org/10.1016/j.conbuildmat.2015.12.171
[4] Limbachiya MC, Leelawat T, Dhir RK (2000) Use of recycled concrete aggregate in high-strength concrete. Mat Struct 33:574–580. https://doi.org/10.1007/BF02480538
[5] CEMBUREAU, CEMBUREAU Activity Report 2021
[6] Etxeberria M, Vázquez E, Marí A, Barra M (2007) Influence of amount of recycled coarse aggregates and production process on properties of recycled aggregate concrete. Cement and Concrete Research 37:735–742. https://doi.org/10.1016/j.cemconres.2007.02.002
[7] Behera M, Bhattacharyya SK, Minocha AK, et al (2014) Recycled aggregate from C&D waste & its use in concrete – A breakthrough towards sustainability in construction sector: A review. Construction and Building Materials 68:501–516. https://doi.org/10.1016/j.conbuildmat.2014.07.003
[8] Silva RV, de Brito J, Dhir RK (2015) The influence of the use of recycled aggregates on the compressive strength of concrete: a review. European Journal of Environmental and Civil Engineering 19:825–849. https://doi.org/10.1080/19648189.2014.974831
[9] Chakradhara Rao M, Bhattacharyya SK, Barai SV (2011) Influence of field recycled coarse aggregate on properties of concrete. Materials and Structures 44:205–220. https://doi.org/10.1617/s11527-010-9620-x
[10] Silva RV, de Brito J, Dhir RK (2015) Tensile strength behaviour of recycled aggregate concrete. Construction and Building Materials 83:108–118. https://doi.org/10.1016/j.conbuildmat.2015.03.034
[11] Ismail S, Kwan WH, Ramli M (2017) Mechanical strength and durability properties of concrete containing treated recycled concrete aggregates under different curing conditions. Construction and Building Materials 155:296–306. https://doi.org/10.1016/j.conbuildmat.2017.08.076
[12] Kisku N, Joshi H, Ansari M, et al (2017) A critical review and assessment for usage of recycled aggregate as sustainable construction material. Construction and Building Materials 131:721–740. https://doi.org/10.1016/j.conbuildmat.2016.11.029
[13] Kim Y, Hanif A, Kazmi SMS, et al (2018) Properties enhancement of recycled aggregate concrete through pretreatment of coarse aggregates – Comparative assessment of assorted techniques. Journal of Cleaner Production 191:339–349. https://doi.org/10.1016/j.jclepro.2018.04.192
[14] Balagopal V, Panicker AS, Arathy MS, et al (2022) Influence of fibers on the mechanical properties of cementitious composites - a review. Materials Today: Proceedings 65:1846–1850. https://doi.org/10.1016/j.matpr.2022.05.023
[15] Polypropylene Fibre-Reinforced Concrete - an overview | ScienceDirect Topics. https://www.sciencedirect.com/topics/engineering/polypropylene-fibre-reinforced-concrete. Accessed 11 Dec 2024
[16] Tošić N, Peralta Martínez D, Hafez H, et al (2022) Multi-recycling of polypropylene fibre reinforced concrete: Influence of recycled aggregate properties on new

concrete. Construction and Building Materials 346:128458. https://doi.org/10.1016/j.conbuildmat.2022.128458
[17] CEN (2022) Tests for mechanical and physical properties of aggregates - Part 6: Determination of particle density and water absorption
[18] Amario M, Rangel CS, Pepe M, Toledo Filho RD (2017) Optimization of normal and high strength recycled aggregate concrete mixtures by using packing model. Cement and Concrete Composites 84:83–92. https://doi.org/10.1016/j.cemconcomp.2017.08.016
[19] CEN (2004) Design of concrete structures - Part 1-1: General rules and rules for buildings
[20] CEN (2005) Test method for metallic fibered concrete - Measuring the flexural tensile strength (limit of proportionality (LOP), residual)
[21] Alberti MG, Enfedaque A, Gálvez JC (2015) Comparison between polyolefin fibre reinforced vibrated conventional concrete and self-compacting concrete. Construction and Building Materials 85:182–194. https://doi.org/10.1016/j.conbuildmat.2015.03.007
[22] Kazmi SMS, Munir MJ, Wu Y-F, Patnaikuni I (2018) Effect of macro-synthetic fibers on the fracture energy and mechanical behavior of recycled aggregate concrete. Construction and Building Materials 189:857–868. https://doi.org/10.1016/j.conbuildmat.2018.08.161
[23] Liu G, Hunger M, Tošić N, De La Fuente A (2023) Effect of free and embedded polypropylene fibres recovered from concrete recycling on the properties of new concrete. Construction and Building Materials 409:134145. https://doi.org/10.1016/j.conbuildmat.2023.134145
[24] Xu F, Li Z, Li T, Wang S (2024) The Mechanical Properties and Microstructure of Tailing Recycled Aggregate Concrete. Materials 17:1058. https://doi.org/10.3390/ma17051058
[25] Lin C, Kanstad T, Jacobsen S, Ji G (2023) Bonding property between fiber and cementitious matrix: A critical review. Construction and Building Materials 378:131169. https://doi.org/10.1016/j.conbuildmat.2023.131169
[26] Liu G, Claramunt J, Hunger M, et al (2024) Effect of coarse recycled aggregate with embedded fibres on the mechanical properties and microstructure of polypropylene fibre-reinforced concrete. Mater Struct 57:241. https://doi.org/10.1617/s11527-024-02527-3